J. Fluid Mech. (1977), *vol.* 79, *part* 4, *pp.* 769–784
Printed in Great Britain

Flow oscillations in a duct with a rectangular cross-section

By J. S. ANDERSON,† W. M. JUNGOWSKI,‡
W. J. HILLER AND G. E. A. MEIER
Max-Planck-Institut für Strömungsforschung, Germany

(Received 14 June 1976)

A two-dimensional configuration has been investigated in which air flows through a convergent nozzle and expands abruptly into a rectangular duct of larger cross-section which terminates in a plenum chamber. Three different types of oscillation have been observed in the downstream duct. At low plenum-chamber pressures an oscillation occurs towards the exit of the duct as the boundary layer of the flow becomes alternately separated and attached. At increasing plenum pressure a shock-pattern oscillation takes place in which a change from a normal shock to oblique shocks occurs during a cycle. At still greater plenum pressures a base-pressure oscillation occurs which influences the entire duct flow downstream of the abrupt change in cross-section. The amplitudes of the oscillation can be as high as 10 % of the rest state, and the frequency of the base-pressure oscillations can be predicted approximately from one-dimensional gasdynamic theory.

The unsteady duct phenomena have been studied by synchronizing instantaneous pressures measured by quartz pressure transducers with interferograms obtained with a Mach–Zehnder interferometer.

1. Introduction

In mixed subsonic and supersonic flow fields an interaction between a shock wave and a boundary layer can take place. As a result of the interaction, separation of the flow may occur and oscillations may begin as the position of the separation point and the shock strength vary during a cycle. Such flow oscillations with similar mechanisms have been observed with widely different flow geometries. Examples include the flow over an aerofoil profile (Dvorak 1964; Karashima 1961; Meier & Hiller 1968; Naumann 1965; Trilling 1958), the flow along a spike on a blunt body (Bogdonoff & Vas 1959; Holden 1966; Maull 1960) and the flow in the intake diffuser of a turbo-jet engine (Dailey 1955). Shock oscillations can also occur when a supersonic jet impinges on a rigid surface (Ginzburg *et al.* 1970; Mørch 1964). Shock-induced flow oscillations have been studied in detail in curved channels and Laval nozzles with rectangular cross-sections (Meier 1974, 1975, 1976). Similar instabilities have been observed in circular ducts following a sudden enlargement (Anderson & Williams 1968;

† Present address: Department of Mechanical Engineering, The City University, London.

‡ Present address: Warsaw Technical University.

Jungowski 1967, 1968, 1969), and in these cases the oscillation resulted in considerable external noise (Anderson 1972; Witczak 1975).

The aim of the present paper is to report on a study of shock-induced flow oscillations in a duct with a sudden enlargement which has a rectangular rather than a circular cross-section. A rectangular duct is more suitable than a circular duct for visualization of the flow patterns by high-speed interferometry. The dimensions of the rectangular duct used were comparable to those of circular ducts which were known to exhibit instabilities. Different types of oscillation have been classified and mechanisms proposed which, it is hoped, will lead to a better understanding of these complicated phenomena.

2. Experimental arrangement

A schematic diagram of the air flow system is shown in figure 1. Atmospheric air, with a temperature between 17 and 20° C and a relative humidity which varied between 20 and 40 %, passed through a short intake (1) to a convergent nozzle (2). This nozzle was about 20 mm in length and was designed to produce a thin boundary layer at the exit. The test duct (3), which is immediately downstream of the nozzle, has a larger cross-section so that the flow suffers an abrupt expansion. After the test section is a plenum chamber (4), the pressure in which can be maintained constant by operation of a control valve (5). The plenum chamber can be quickly connected to a vacuum chamber of volume 132 m^3 (7) by a pneumatically operated gate valve (6). The width of the nozzle, test duct and plenum chamber was constant and equal to 100 mm.

The flow field in the test duct was studied with the aid of an interferometer of the Mach–Zehnder type. The light source was a spark in a chamber of argon and had a duration of 1 μs. Interferograms could be obtained at a frame rate of 10 kHz using a high-speed drum camera. (More details of the optical arrangements can be obtained from Meier & Hiller 1968.) Light passed through optical windows whose positions are shown in figure 1 in relation to the test duct. The interference fringes in the interferograms are lines of constant density, and if the flow field is isentropic other state variables, such as pressure and temperature, are also constant along the fringes.

Pressure fluctuations can be measured by quartz piezo-electric transducers placed on the upper or lower surface of the duct. Traces of pressure against time were obtained by an ultra-violet light recorder, but because the frequency of the pressure oscillation was too high for clear resolution the signals were first recorded on magnetic tape by an Ampex FM recorder and replayed to the light recorder at a lower speed. Static pressures at the duct walls were measured by precision aneroid manometers and by mercury manometers.

The main geometrical parameters of the duct are the nozzle height h, test-duct height H and test-duct length L. The nozzle height could be varied and was mostly maintained between 6 mm and 18 mm for the experiments described in this paper. The height of the duct was varied between 25 mm and 50 mm, and duct lengths of 80, 160, 240 and 320 mm were used. Area ratios ϕ ($= h/H$) of from 0·2 to 0·5 were tested.

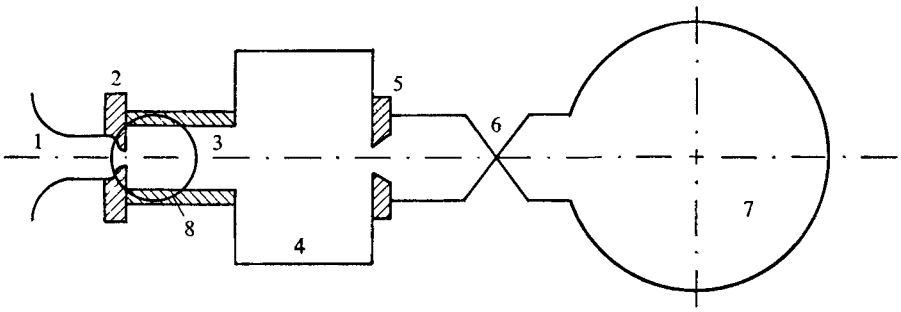

FIGURE 1. Schematic diagram of experimental arrangement. 1, intake; 2, nozzle; 3, test duct; 4, plenum chamber; 5, throttle valve; 6, gate valve; 7, vacuum chamber; 8, optical window.

3. Classification of flow patterns and related pressure conditions

In this section the different flow patterns and modes of oscillation are related to the static pressure conditions.

Figure 2 shows the influence of the plenum-chamber pressure p_e on the time-averaged pressure $\overline{p}_w$ in the base region or dead air at the upstream corners of the duct. In figure 2 (*a*), which refers to a relatively short duct with $L = 160$ mm and $H = 33{\cdot}2$ mm, the base pressure remains constant for low plenum-chamber pressure p_e, but for values of p_e/p_a, where p_a is the atmospheric pressure, above 0·25 the base pressure increases. In the range of plenum-chamber pressure ratios 0·305–0·352 a large amplitude oscillation in the base-pressure region can occur. When these oscillations exist the base pressure is low, and the flow is symmetrical. With plenum-chamber pressure ratios from 0·316 to 0·352 an additional flow pattern may occur in which the flow is asymmetrical, but steady, and attached to either the top or bottom surface of the duct. For this second flow pattern there is no preferred attachment to either the top or bottom surface. During an experiment the flow may attach to, say, the top surface and remain attached to that surface as long as the asymmetrical flow pattern is allowed to exist. If, however, the duct is closed down and then restarted attachment may occur on the lower surface. For this asymmetrical flow there are two base pressures, a lower value for the attached side and a higher value for the unattached side. Thus, in the plenum pressure ratio range 0·316–0·352 three different values of the base pressure are recorded in figure 2 (*a*).

The existence of one or other of the two possible flow patterns depends upon whether the plenum-chamber pressure is increasing or decreasing. As the plenum-chamber pressure ratio increases from 0·305 to 0·352 the oscillating flow pattern exists, but at a pressure ratio of 0·352 the base pressure suddenly increases and the flow pattern switches to the asymmetrical steady form. With decreasing plenum pressure the steady pattern exists down to a pressure ratio of 0·316, when the oscillation suddenly starts and the base pressure decreases. The resulting hysteresis is indicated in figure 2 (*a*) by the arrows.

In figure 2 (*b*) the geometric parameters are the same as in figure 2 (*a*), apart from the duct length L, which is now 240 mm, but the pressure conditions have

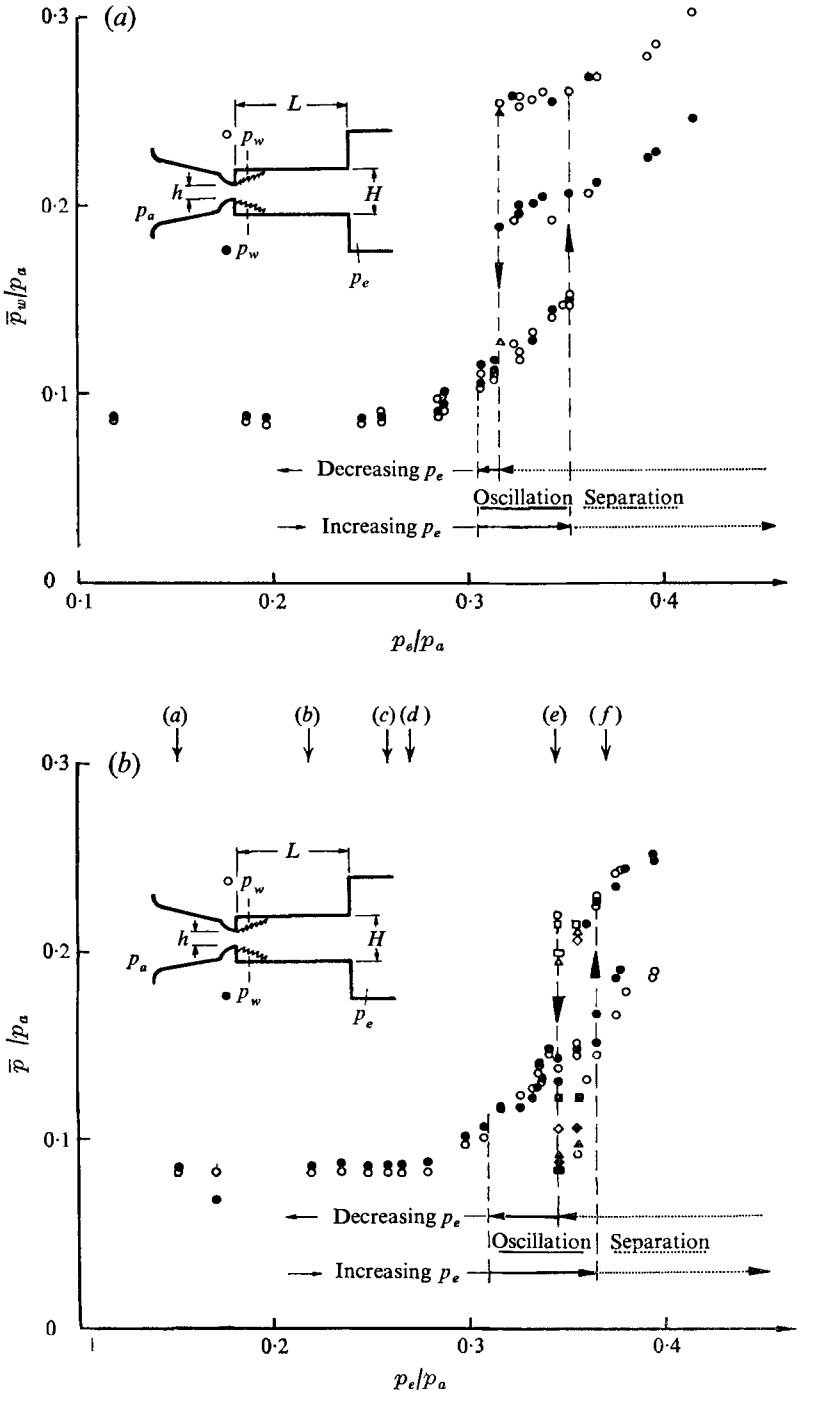

FIGURE 2. Variation of base pressure with receiver pressure. $\phi = 0{\cdot}3$, $h = 10$ mm, $H = 33{\cdot}2$ mm. (*a*) $L = 160$ mm, (*b*) $L = 240$ mm. (Solid and open symbols represent different pairs of values of $\overline{p}_w$ for different tests.)

some differences. For values of p_e/p_a up to 0·28 the base pressure is constant and has nearly the same value as that recorded in figure 2 (*a*) for low plenum pressures. In this range of constant base pressure the flow (downstream of the reattachment close to the nozzle) is entirely supersonic, and an interferogram of this steady supersonic flow is shown as figure 3(*a*) (plate 1) for a plenum pressure ratio of 0·151. (It should be noted that because of the restricted field of view of the optical windows the downstream part of the duct cannot be included.)

The interferogram in figure 3(*a*) shows the supersonic flow to be divided into cells by crossing oblique shock waves. At the reflexion of the shock waves at the duct wall the boundary layer is thickened, but there is no major separation from the walls. Closer to the nozzle, in the reattachment region of the jet, the first oblique shock waves are formed from the reflexion of the expansion waves generated at the nozzle exit. The dead, or trapped, air in the corners of the duct near the nozzle can be seen, and is limited by the duct walls and jet boundaries. The vorticity in the trapped air was made visible because of distortions in the thickness of a thin oil film on the windows which was present only in the corners of the duct.

Figure 3(*b*) (plate 1) corresponds to a plenum pressure ratio of 0·219, and although the base pressure still has the minimum value, the flow is no longer steady. Separation of the flow occurs on both sides of the duct, resulting in distortions of the shock-wave pattern and the generation downstream of the separation points of new oblique shock waves not seen in figure 3(*a*). The unsteady behaviour of the jet-like structure behind the separation leads to an irregular pressure oscillation in the downstream part of the duct. This type of unsteady flow is referred to as a 'downstream random oscillation of the separated supersonic flow'. The pressure variation can be detected by pressure transducers located in the downstream part of the duct, but the pressure upstream of separation and in the base region is steady.

At a plenum pressure ratio of 0·258 the flow is still unstable, but the instability is of a different kind. Figure 3(*c*) (plate 1) is an interferogram of the flow at an instant during the oscillation cycle. This type of oscillation is characterized by a change in the shock structure during a cycle from crossing oblique shocks to a normal shock. The base pressure remains steady and the changes in the flow pattern take place in the region downstream of attachment. This mode of oscillation is referred to as a 'shock-pattern oscillation'. The ranges of pressure ratios for the downstream oscillation and the shock-pattern oscillation are connected. The combined range of plenum pressure ratios is 0·16–0·26.

As the plenum pressure ratio is increased above 0·26 the oscillations disappear. Figure 3(*d*) (plate 1), for a pressure ratio of 0·265, is an example of this stable flow. Behind the strong, normal shock wave in the centre of the duct is a subsonic flow, whilst small supersonic flow regions are attached to both the walls of the duct. The supersonic regions start at branched shock waves at the upper and lower extremities of the normal shock. Thus in this case the central flow behind the shock always has a lower Mach number than the outer flow, and in addition the boundary layer in the region of the shocks cannot be seen to separate. Supersonic flow upstream of the shock-wave system indicates that the duct

flow in this region is choked, and hence no disturbances can travel upstream to the base-pressure region, other than weak disturbances in the subsonic part of the boundary layer.

In figure 3(*e*) (plate 1) the plenum pressure ratio has increased considerably to 0·345, but the interferogram does not appear to be greatly different from figure 3(*d*). There is, however, one important difference: the flow upstream of the shock waves is subsonic at the boundaries, whereas in figure 3(*d*) the flow in this region was supersonic. In figure 3(*e*) there is no density maximum upstream of the shocks nor do the shock waves stretch entirely across the duct, and it is on these two reasons that the difference between figures 3(*d*) and (*e*) is based.

The presence of the subsonic flow upstream of the shock is important, because it is now possible for disturbances to travel upstream to the base-pressure region. At a plenum pressure ratio of 0·345 large amplitude oscillations of the base pressure occur and figure 3(*e*) is just one picture of the changing flow pattern during the oscillation. For $L = 240$ mm and $\phi = 0{\cdot}3$ the large amplitude oscillations occur over a range of plenum pressure ratios of 0·31–0·365; they are called in this paper 'base-pressure oscillations' and have already been mentioned in relation to figure 2 as the main type of oscillation. It is believed that similar oscillations can occur in circular ducts with sudden enlargements (Jungowski 1969; Witczak 1975).

Figure 3(*f*) (plate 1) corresponds to a plenum-chamber pressure ratio of 0·375 and the flow field has now separated entirely from one side of the duct. The interferogram shows a supersonic jet with a cellular structure which becomes subsonic downstream of the attachment area. With the asymmetrical flow fields weak random oscillations can occur, but with higher area ratios a new kind of stronger oscillation, which is related to the base-pressure type, is often able to exist. These one-sided base-pressure oscillations are described at the end of the next section.

4. Interferogram sequences and pressure–time traces

The previous section described single pictures typical of the different flow patterns but, as the interferograms can change during a cycle, a more complete view can be obtained only from a sequence of photographs during a cycle. The high-speed photographs shown here were taken at a frame rate of 10 kHz, but some pictures were omitted from the sequences to leave twelve pictures at equal time intervals during the cycle. With each picture sequence, traces of pressure Δp *vs.* time Δt are shown which have been obtained from measurements by transducers at the positions indicated. A series of superimposed impulses can be seen on the pressure traces at the end of the records and each impulse corresponds to a photograph taken at a frame rate of 10 kHz. In this way synchronization of the interferograms and the pressure fluctuations is possible.

The first sequence of interferograms, taken at an effective frame rate of 2·5 kHz, is shown in figure 4 (plate 2) for a duct of area ratio 0·3 and length 160 mm. The plenum-chamber pressure ratio is 0·255 and the overall statci

pressure conditions can be studied in figure 2(*a*). Figure 4 shows one cycle of the shock-pattern oscillation.

The instantaneous pressure at transducer position 3 for frame 1 can be seen to have a low value. Separation takes place symmetrically on either side of the duct and oblique shock waves are generated at the points of separation. Downstream of separation the central flow is slightly supersonic and the separated flow near the boundaries is subsonic. By frame 3 the pressure is starting to increase and the separation points move upstream, the separated flows becoming more asymmetrical.

Frame 4 shows the emergence of two normal shock waves. The upstream normal shock starts to form at the intersection of the oblique shocks generated by the reflexion of the expansion fans. The downstream normal shock is formed at the intersection of the oblique shocks created near the flow separation points. These two normal shocks move towards each other and eventually combine (in frame 7) when the pressure at position 3 is a maximum. The flow field now has a subsonic central core and supersonic side flows; this pattern is the reverse of that existing at low pressures in frame 1. The flow pattern remains similar from frame 7 to frame 10, when rapid downstream motion of the separation points begins, and by frame 12 the low pressure flow pattern, with the supersonic central part, has been reconstituted.

During the shock-pattern type of oscillation there is an interaction between the central flow field and the separated region which is controlled by intermixing of the central and outer regions and by the transverse pressure gradient.

The pressure traces in the lower section of figure 4 show the oscillations to be random, but the sequence chosen is considered to be reasonably typical. The average frequency of the oscillations is 167 Hz. The two lower pressure traces of figure 4 also show that the pressure upstream of the region of the shock-pattern oscillation is not varying.

Figure 5 (plate 3) refers to the same duct as figure 4 ($\phi = 0{\cdot}3$, $L = 160\,\text{mm}$), but the value of p_e/p_a has been increased to 0·348. As the plenum pressure ratio is increased from that corresponding to figure 4 the shock-pattern oscillation ceases and the flow is stable for a small range of pressures until the large amplitude base-pressure oscillations begin; these then continue until a pressure ratio of 0·352. The traces in the lower part of figure 5 show a major characteristic of the base-pressure oscillations: a strong cyclical variation recorded by all four transducers, including those in the dead-air region. The frequency of the oscillation is 373 Hz. Evidence to be cited later indicates that the oscillation is controlled by the resonant frequency of the duct, which is to some extent affected by the Mach number in the duct.

The interferograms for the base-pressure oscillations shown in figure 5 were taken at an effective frame rate of 5 kHz. In frame 1 the dead-air region is connected to the downstream region by a subsonic layer on both sides of a central supersonic flow near the nozzle exit. The supersonic flow ends with a strong normal shock which is followed by subsonic flow in the central part of the field. Supersonic layers are formed downstream of the extremities of the normal shock and surround the central subsonic region. These patterns of supersonic flow are

more clearly visible in frames 2 and 3. The phases in frames 1–3 correspond to low pressure at transducer position 3, and are connected with high outer velocities in the separated flow field. Thus there is entrainment of air from the base-pressure region through the space between the bounding walls and the supersonic layers. Pressure traces in the base-pressure region, at positions 1 and 7, show a decrease during this time.

From frame 3 to frame 6 the normal shock is moving upstream, reaching a position closest to the nozzle in frame 6. The minimum base pressure is reached a little earlier, in frame 4, after which the base pressure increases as the pressure ratio across the normal shock also increases. From frame 4 to frame 10 the base pressure continues to increase and, as a consequence of the reducing expansion angle of the supersonic nozzle flow, the height of the separated supersonic flow field in the centre is reduced. As a result this separated flow field becomes more jet-like with higher Mach numbers downstream of the shock wave and decreasing pressure values at transducer locations 3 and 5.

From frame 8 to frame 12 the strength of the shock wave decreases, its height is reduced and its position moves downstream. Thus during the cycle the shock strength and location alternate, with accompanying changes in the downstream flow patterns.

The base-pressure oscillations described above can be referred to as symmetrical in that their amplitudes are of the same order in the two corners of the duct. Large amplitude base-pressure oscillations in asymmetrically attached flows have also often been observed and figure 6 (plate 4) shows some typical examples for an area ratio of 0·4 and duct length of 240 mm. With this configuration the asymmetrical flow is formed when p_e/p_a is greater than 0·4.

Figure 6(*a*) shows a flow pattern for a plenum-chamber pressure ratio of 0·42 in which the main nozzle exit flow is attached to the upper boundary of the duct. (It should be re-emphasized here that there is no preferred attachment surface, and attachment could just as easily have occurred on the lower surface.) Pressure traces indicate a fairly regular oscillation at a frequency of 165 Hz which has a small amplitude in the upper base-pressure region (transducer position 7). In this case the oscillation mechanism is acting only on the lower side of the jet. Some similarities of this oscillation flow field with the flow fields of figure 5 allow us to deduce that the mechanism is like a one-sided base-pressure oscillation in which the upper, attached supersonic flow is unaffected. Thus the main flow provides screening for the upper, steady flow. The interferogram in figure 6(*a*) is just one picture in a cycle in which the flow field in the central part of the jet is subsonic, but is surrounded by supersonic outer layers, the upper of which is attached to the walls.

The one-sided base-pressure oscillation on the unattached side, as described above, existed for values of p_e/p_a from 0·4 to 0·44.

With a further increase in the plenum-chamber pressure ratio to 0·48 the centre of the oscillation is switched to the upper boundary. The flow pattern for this pressure ratio, shown in figure 6(*b*), once again has the main flow attached to the upper side of the duct, but the pressure traces show a considerable change in amplitude and relative phase. The main flow remains supersonic for a relatively

long distance, but is of reduced height. The primary flow is always far from the lower boundary, and the extensive subsonic flow between the main jet and the lower boundary prevents the base-pressure type of oscillation. The corresponding pressure traces show a regular oscillation of frequency 256 Hz at the base on both sides of the nozzle (transducer positions 1 and 7), although that at transducer position 7 has the greater amplitude. The amplitudes at the downstream positions (3 and 8) are also less than the amplitudes at 7.

In the type of oscillation shown in figure 6(*b*) the cellular pattern of the main flow near the nozzle is closely involved in the oscillation mechanism. This form of oscillation associated with the cellular structure exists for values of p_e/p_a from 0·48 to 0·503. Another example of the same type, at $p_e/p_a = 0{\cdot}488$, is shown in figure 6(*c*), where the frequency of oscillation is 241 Hz.

The frequencies of oscillation in figure 6 are all of the same order, and because of this it can be concluded that the same duct resonance mode supports the different types of oscillation mechanism.

5. Time sequences of density

Density distributions along the axis of the duct and at the boundary are shown in figures 7(*a*) and (*b*), respectively. The letters next to the curves correspond to those in figure 3. ρ is the density in the duct and ρ_a is the density of the atmosphere. In the figures x is the distance downstream from the middle of the nozzle exit and y is the perpendicular distance from the duct centre-line. Note that the origin for the ordinate is different for each curve. The main oscillation cases (*c*, shock-pattern oscillation; *e*, base-pressure oscillation) show a steeper density increase in the downstream part of the flow field than the steady cases (*a*, *d*, *f*). This increase can be more exactly demonstrated by taking a time average of the density variations in one cycle for a similar configuration (see figure 8). Figures 8(*a*) and (*b*) show density distributions for one instant of time during an oscillation cycle of the shock-pattern type for the twelve frames shown in figure 4. The density curves 1–6 show disturbances travelling against the flow in the downstream section of the duct. These disturbances increase the strength and shift the position of the shock wave at the end of the main supersonic flow regime. The influence of the oscillation and the motion of the disturbances on the boundary flow, as seen in figure 8(*b*), is not very strong but is visible in curves 4 and 5.

The base-pressure oscillation of figure 5 has density sequences which have been plotted in figure 9. The density distribution along the axis (figure 9*a*) clearly shows the motion of the shock wave during the oscillation cycle. The distribution at the boundary (figure 9*b*) shows a monotonic density increase for the whole duct. Only small disturbances occur in this area.

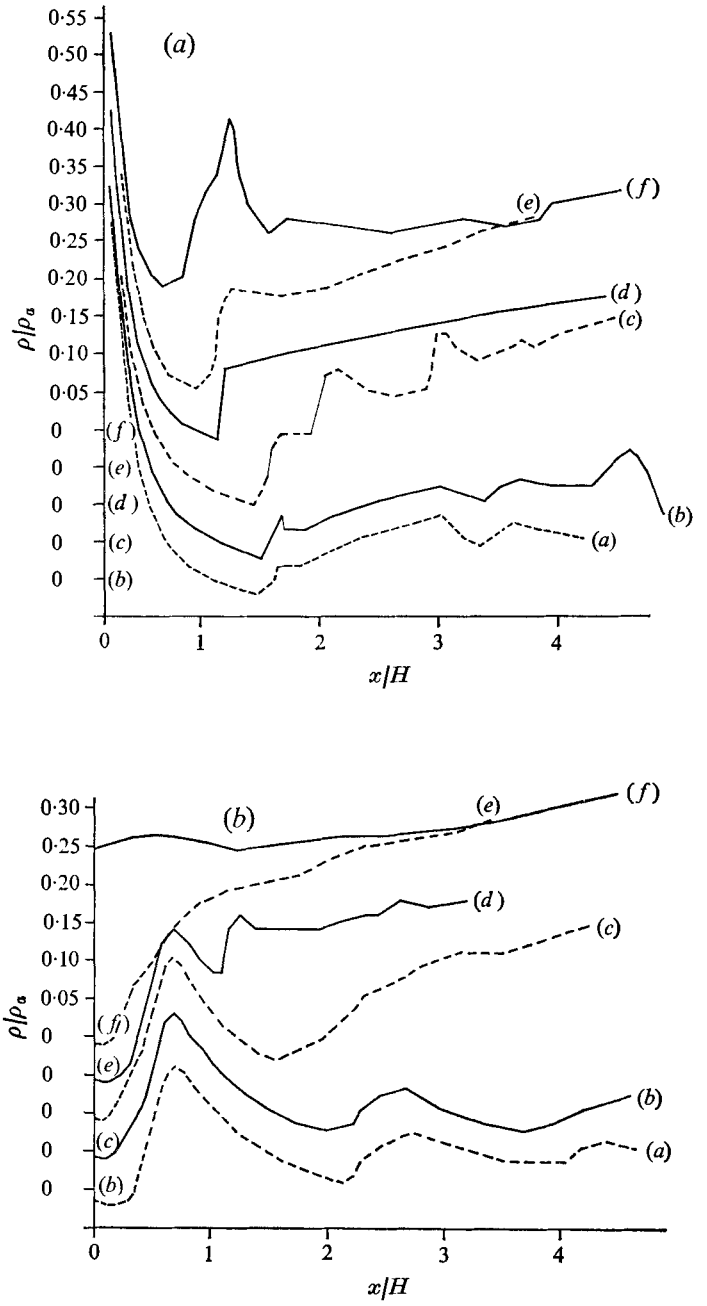

FIGURE 7. Streamwise density distributions in the duct. $\phi = 0{\cdot}3$, $L = 240$ mm. (*a*) $y = 0$ (on the axis), (*b*) $y = -0{\cdot}45H$ (close to the wall).

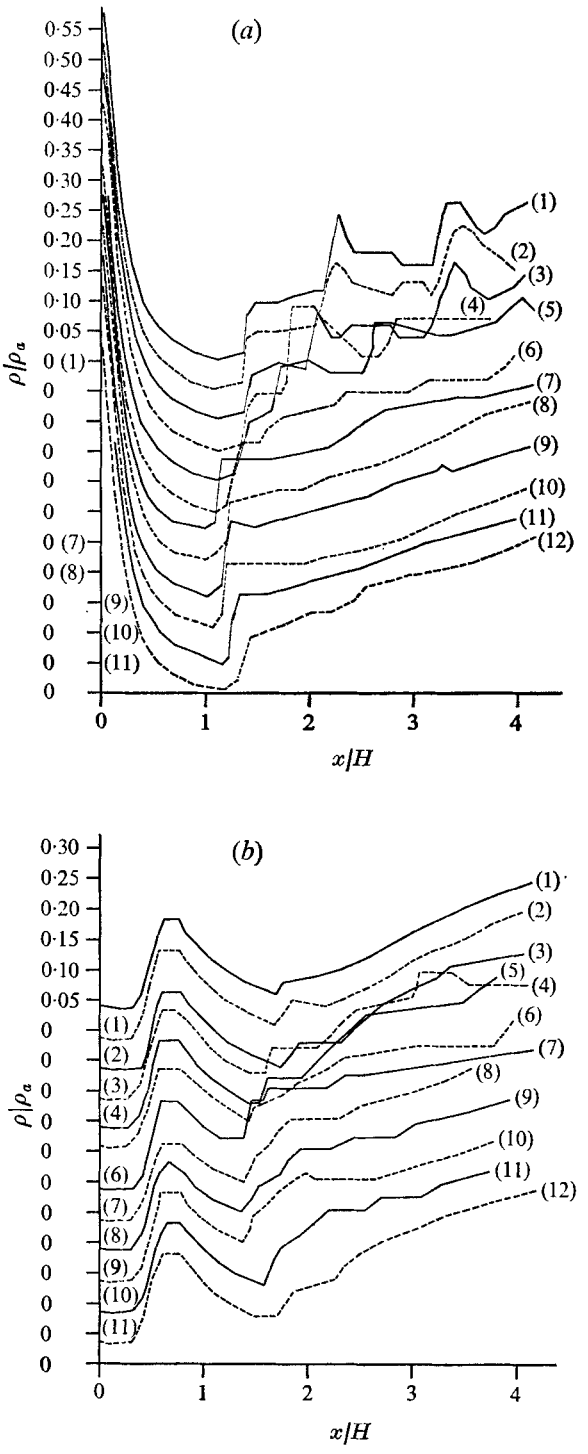

FIGURE 8. Sequences of streamwise density distributions for the shock-pattern oscillation. $\phi = 0{\cdot}3$, $L = 160$ mm. (*a*) $y = 0$ (on the axis), (*b*) $y = -0{\cdot}45H$ (close to the wall).

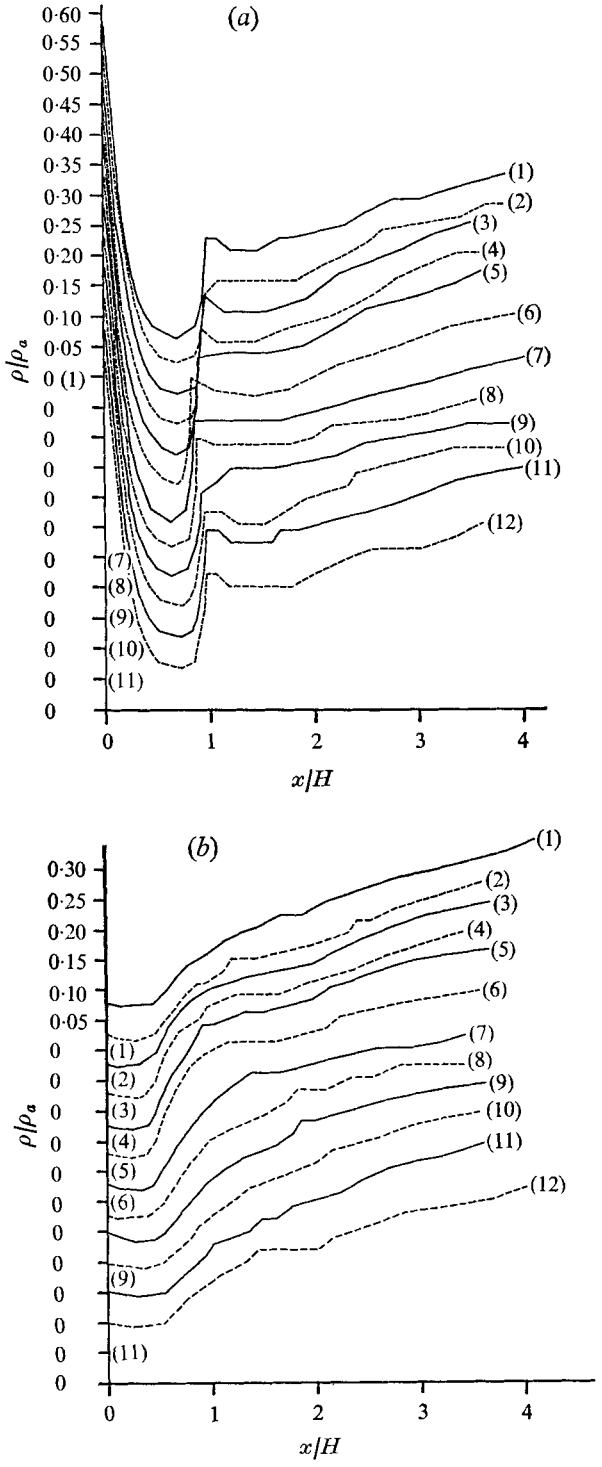

FIGURE 9. Sequences of streamwise density distributions for the base-pressure oscillation. $\phi = 0{\cdot}3$, $L = 160$ mm. (*a*) $y = 0$, (*b*) $y = -0{\cdot}45\,H$.

6. Influence of controlling parameters

The parameter sets which were investigated are shown in figure 10. The black triangles indicate occurrence of a strong base-pressure oscillation.

The range of pressure ratios corresponding to the main type of oscillation, i.e. the base-pressure oscillation, is plotted against area ratio ϕ in figure 11 for the rectangular ducts tested in the present series of experiments and for circular ducts investigated previously (Witczak 1975). With rectangular ducts the upper boundary of the average base pressure, indicated by dash–dot lines, has a steeper increase than the lower boundary, which is shown as a dashed line. The base pressures corresponding to oscillations of both the symmetrical and the asymmetrical kind in the rectangular duct lie within the area between the curves. In the case of base-pressure oscillations of the asymmetrical kind each condition is represented by a pair of points, one for the low pressure side and the other for the high pressure side. With symmetrical flow the base pressures are equal on both sides and the corresponding point is located in the lower part of the range. The curve below the oscillation range (drawn through the triangular points) gives the minimum pressure ratio for steady conditions in the dead-air region.

The range of oscillation is smaller for circular ducts than for the rectangular case because with circular ducts only symmetrical oscillations take place, and thus the asymmetrical oscillations in the upper part of the range are not present.

Experimental evidence shows a strong dependence of frequency upon duct length. The natural frequencies of longitudinal oscillations in the duct have been estimated in order to show that the base-pressure oscillations are controlled by duct resonance. The resonant frequency of the air in the duct is affected by the velocity of the mean flow, which can be estimated from a one-dimensional approach. The equations of continuity, momentum and energy, when applied to an abruptly expanding sonic flow, give (Jungowski 1968)

$$\left(\frac{1-\phi}{\phi}\right)\frac{\bar{p}_w}{p_a} = \left(\frac{2}{k+1}\right)^{k+1/2(k-1)} \frac{1+kM^2}{M[1+\frac{1}{2}(k-1)M^2]^{\frac{1}{2}}} - (k+1)\left(\frac{2}{k+1}\right)^{k/(k-1)},$$

where M is a mean subsonic Mach number for the subsonic flow in the duct downstream of the sudden enlargement, and k is the ratio of specific heats. For a given area ratio ϕ, M can be calculated if a value of $\bar{p}_w$ is obtained from measurements. The velocity of sound c in the duct was then obtained from tables of adiabatic flow and a resonant frequency f for the duct was calculated from the formula

$$f = (2n-1)(1-M^2)\,c/4L, \quad \text{for} \quad n = 1, 2, 3, \text{etc.},$$

which gives the resonant frequency of longitudinal oscillations of a duct closed at one end with a mean Mach number of M. Thus a non-dimensional frequency parameter can be obtained: the ratio of the measured frequency f_m of the base-pressure oscillations to the resonant frequency calculated by the above method. In figure 12 this frequency parameter has been plotted against a Strouhal number St_d which is given by

$$St_d = f_m d/u_w,$$

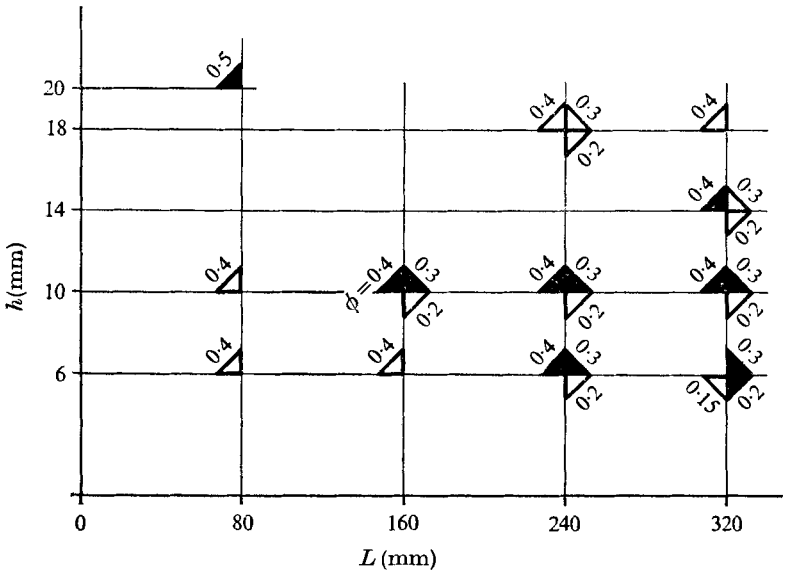

FIGURE 10. Tested sets of geometrical parameters for base-pressure oscillation. ▲, oscillation; △, no oscillation.

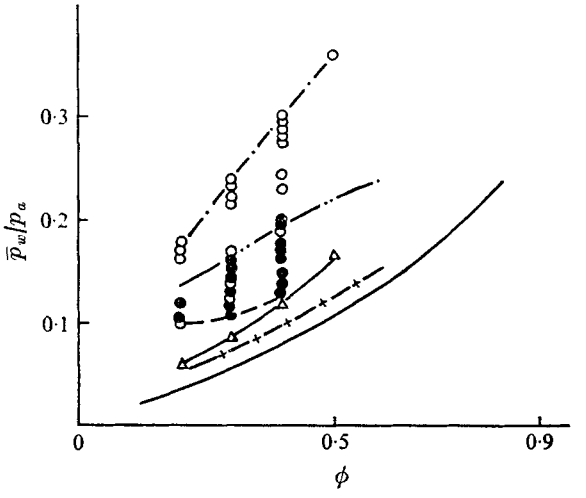

FIGURE 11. Non-dimensional base pressure *vs.* area ratio. —·—, measured upper bound of oscillations for rectangular ducts; ------, measured lower bound of oscillations for rectangular ducts; ○, larger value of base pressure for asymmetric flow; ●, smaller value of base pressure for asymmetric flow; —··—, measured upper bound of oscillations for circular ducts (Witczak 1975); --+--, measured lower bound of oscillations for circular ducts (Witczak 1975); —△—, measured lowest base-pressure limit for rectangular ducts in present tests; ——, lowest base-pressure limit for circular ducts (Witczak 1975).

where $d = \frac{1}{2}(H-h)$, the height of the step of the sudden enlargement, and u_w is the velocity in the duct calculated assuming isentropic expansion from atmospheric pressure p_a to the base pressure $\bar{p}_w$. The ratio of measured to calculated frequencies is close to unity, within -28% to $+7\%$, and varies through a wide range of Strouhal numbers. Figure 12 is taken to indicate

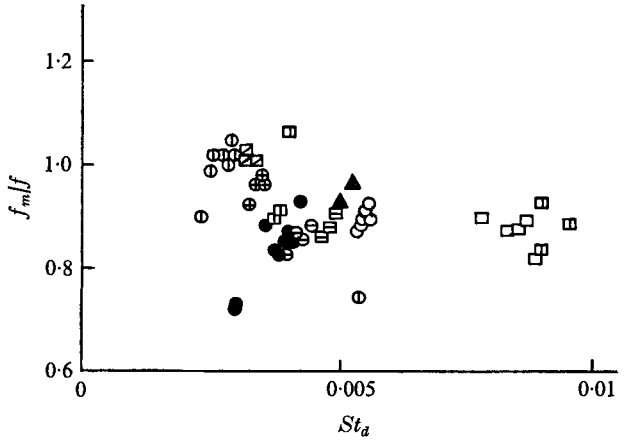

FIGURE 12. Non-dimensional frequency *vs.* Strouhal number for base-pressure oscillations.

	▲	□	◫	⊟	◪	○	ⓘ	●	⊕	⊖
ϕ	0·2	0·3	0·3	0·3	0·3	0·4	0·4	0·4	0·4	0·4
h (mm)	6	10	6	10	6	10	6	10	10	14
L (mm)	320	160	240	320	320	160	240	240	320	320

that the duct length is the most important parameter determining the frequency.

The amplitudes of the base-pressure oscillations are not constant throughout the pressure range. The amplitudes increase with p_e/p_a to a maximum and then suddenly decrease, and indeed the oscillations are often intermittent near the upper pressure limit. The peak-to-peak pressure values vary from 0·06 to 0·24 bars.

Reynolds number effects have not been investigated in any detail, because of the limited range of geometries available with the present apparatus. However, from tests already undertaken it is clear that the boundary-layer thickness at the nozzle exit is a major factor influencing the oscillations. Early experiments with a relatively long converging nozzle, which produced a thick boundary layer, did not induce oscillatory flows in the duct, whereas a short converging nozzle of almost semicircular section successfully produced in the same ducts the oscillations described in this paper. It is intended to study nozzle boundary-layer effects in the future.

7. Conclusions

The mixed supersonic and subsonic flow in a duct with a sudden enlargement in cross-section has three different types of instabilities which lead to oscillations of the flow field. With increasing downstream-receiver pressure downstream oscillations, shock-pattern oscillations and base-pressure oscillations can occur. The most significant is the base-pressure type, where the variations in pressure are large. The base-pressure oscillations can be either symmetrical or one-sided. Between the oscillation regimes there are ranges of static receiver pressure where the flow is stable.

The frequency of the base-pressure oscillations is mainly determined by the length of the duct. The flow oscillation synchronizes with the resonant frequency of longitudinal vibrations of the air in the duct. The mechanism of the flow oscillation is based on a shock-wave/flow-separation interaction which is governed by parameters such as boundary-layer thickness, area ratio and height-to-length ratio. The pressure and density fluctuations are typically 10 % of the stagnation values.

REFERENCES

ANDERSON, J. S. 1972 The noise from abruptly expanded jets. *EUROMECH* 34, *Colloq. Control Feedback Mechanisms in Flow Noise, Göttingen.*

ANDERSON, J. S. & WILLIAMS, T. J. 1968 Base pressure and noise produced by the abrupt expansion of air in a cylindrical duct. *J. Mech. Engng Sci.* **10**, 262–268.

BOGDONOFF, S. M. & VAS, J. E. 1959 Preliminary investigations of spiked bodies at hypersonic speeds. *J. Aero. Space Sci.* **26**, 65–74.

DAILEY, C. L. 1955 Supersonic diffuser instability. *J. Aero. Sci.* **22**, 733–749.

DVORAK, R. 1964 On the unsteady boundary-layer shock wave interaction in the lower transonic region. *Arch. Mech. Stosowanej*, **16**, 211–222.

GINZBURG, I. P., SEMILETENKO, B. G., TERPIGGORIEFF, W. S. & USKOFF, W. N. 1970 Some pecularities resulting from the interaction of a supersonic under-expanded jet with a flat plate. *J. Engng Phys.* **19**, 412–417 (in Russian).

HOLDEN, M. S. 1966 Experimental studies of separated flows at hypersonic speeds. Part 1: separated flows over axi-symmetric spiked bodies. *A.I.A.A. J.* **4**, 591–599.

JUNGOWSKI, W. M. 1967 On the pressure oscillating in a sudden enlargement of a duct section. *Fluid Dyn. Trans.* **1**, 735–741.

JUNGOWSKI, W. M. 1968 Investigation of flow pattern, boundary conditions and oscillation mechanism in a compressible flow through sudden enlargement of a duct. *Warsaw Tech. Univ. Publ.* no. 3.

JUNGOWSKI, W. M. 1969 On the flow in a sudden enlargement of a duct. *Fluid Dyn. Trans.* **4**, 231–241.

KARASHIMA, K. 1961 Instability of shock wave on thin airfoil in high subsonic flow. *Aero. Res. Inst., Univ. Tokyo, Rep.* no. 363.

MAULL, D. J. 1960 Hypersonic flow over axially symmetric spiked bodies. *J. Fluid Mech.* **8**, 584–592.

MEIER, G. E. A. 1974 Ein instationäres Verhalten transsonischer Strömungen. *Mitt. Max-Planck-Inst. Strömungsforsch. Aero. Versuchsanstalt*, no. 59.

MEIER, G. E. A. 1975 Shock-induced flow oscillations. *AGARD Current Paper*, no. 168, pp. 30-1–30-9.

MEIER, G. E. A. 1976 Shock-induced flow oscillations in a Laval nozzle. *Proc. IUTAM Symp. Transonicum* II.

MEIER, G. E. A. & HILLER, W. 1968 An experimental investigation of unsteady transonic flow by high-speed interferometric photography. *AGARD Current Paper*, no. 35.

MØRCH, K. A. 1964 A theory for the mode of operation of the Hartmann air jet generator. *J. Fluid Mech.* **20**, 141–159.

NAUMANN, A. 1965 Stoßschwingungen an Profilen. *Abh. Aero. Inst., TH Aachen*, **18**, 9–13.

TRILLING, L. 1958 Oscillating shock boundary-layer interaction. *J. Aero. Sci.* **25**, 301–304.

WITCZAK, K. J. 1975 Noise caused by sonic flow of gas into a duct. Doctoral thesis, Warsaw Technical University.

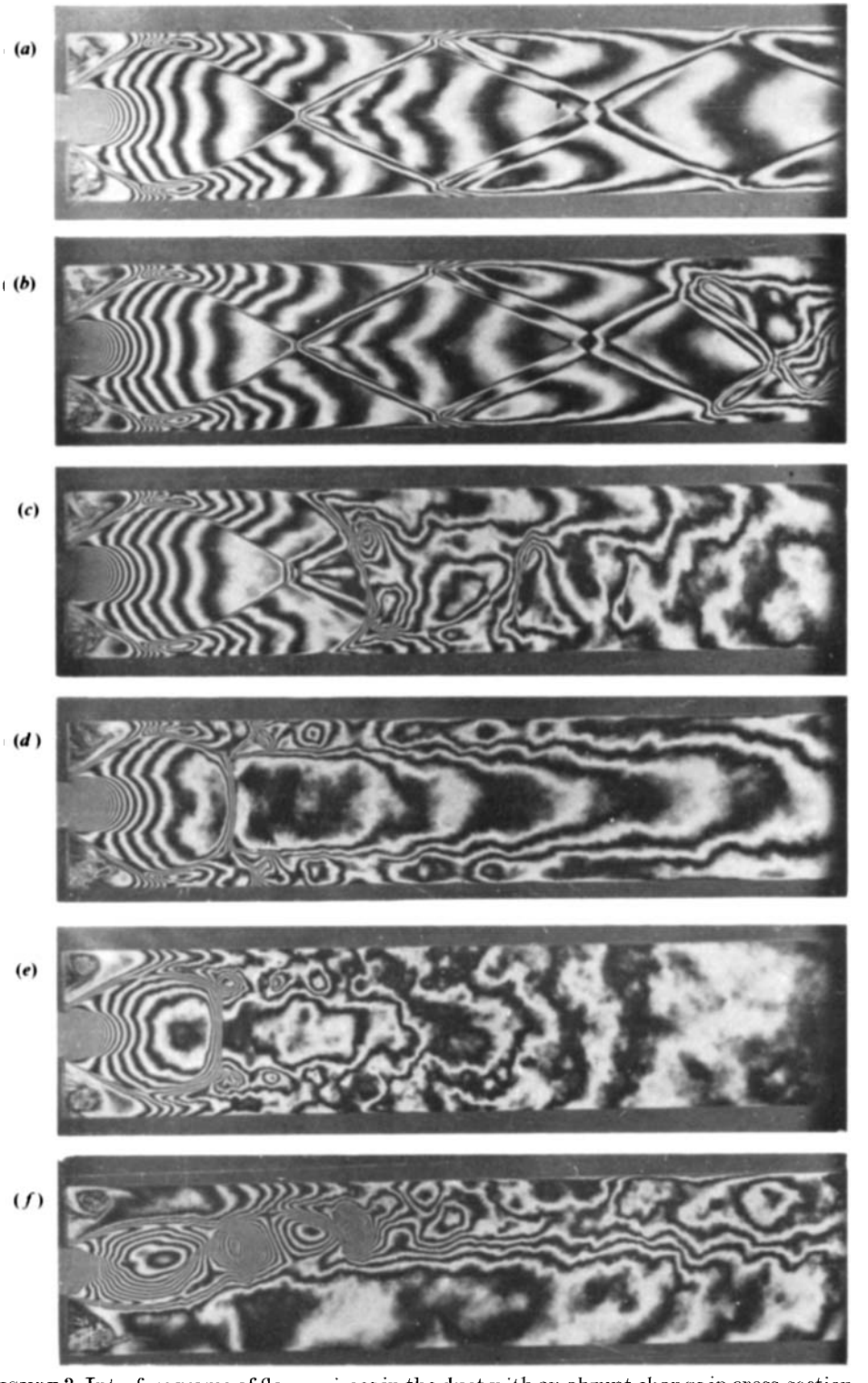

FIGURE 3. Interferograms of flow regimes in the duct with an abrupt change in cross-section. $\phi = 0{\cdot}3, L = 240$ mm. (*a*) $p_e/p_a = 0{\cdot}151$, (*b*) $p_e/p_a = 0{\cdot}219$, (*c*) $p_e/p_a = 0{\cdot}258$, (*d*) $p_e/p_a = 0{\cdot}265$. (*e*) $p_e/p_a = 0{\cdot}345$, (*f*) $p_e/p_a = 0{\cdot}375$.

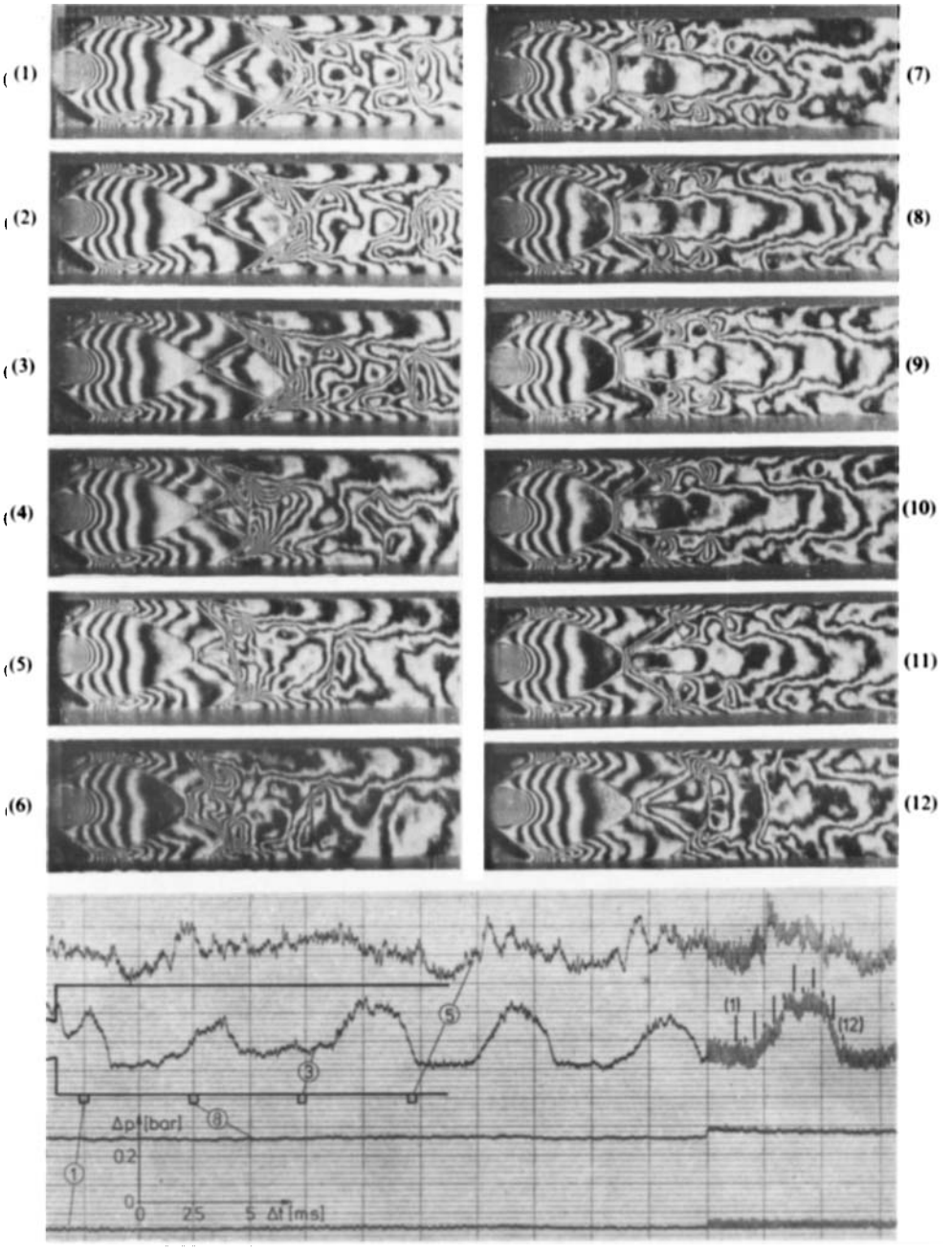

FIGURE 4. Interferogram sequences of a shock-pattern oscillation, with corresponding pressure–time traces. $\phi = 0{\cdot}3$, $L = 160$ mm, $p_e/p_a = 0{\cdot}255$.

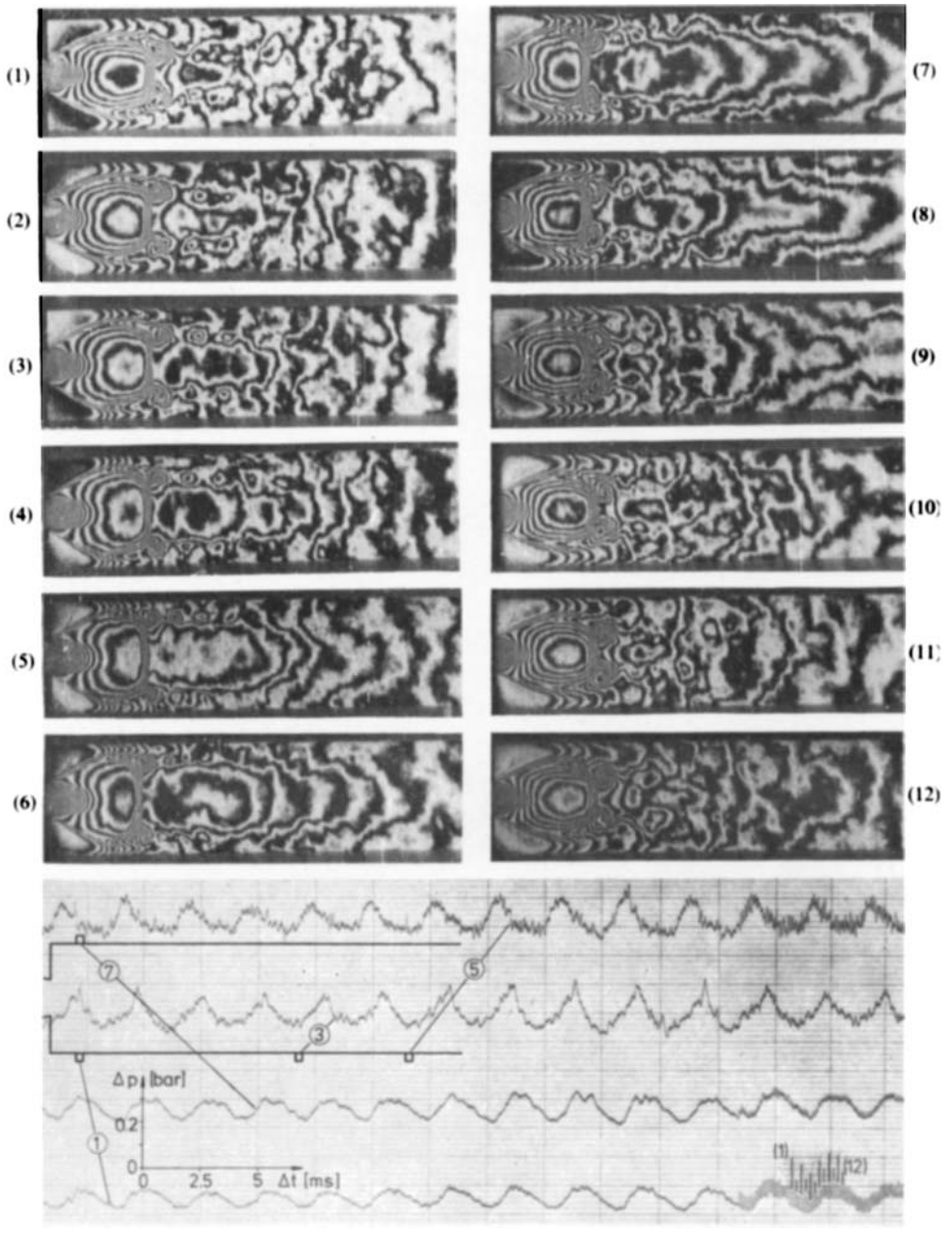

FIGURE 5. Interferogram sequences of a base-pressure oscillation with corresponding pressure–time traces. $\phi = 0{\cdot}3$, $L = 160$ mm, $p_e/p_a = 0{\cdot}348$.

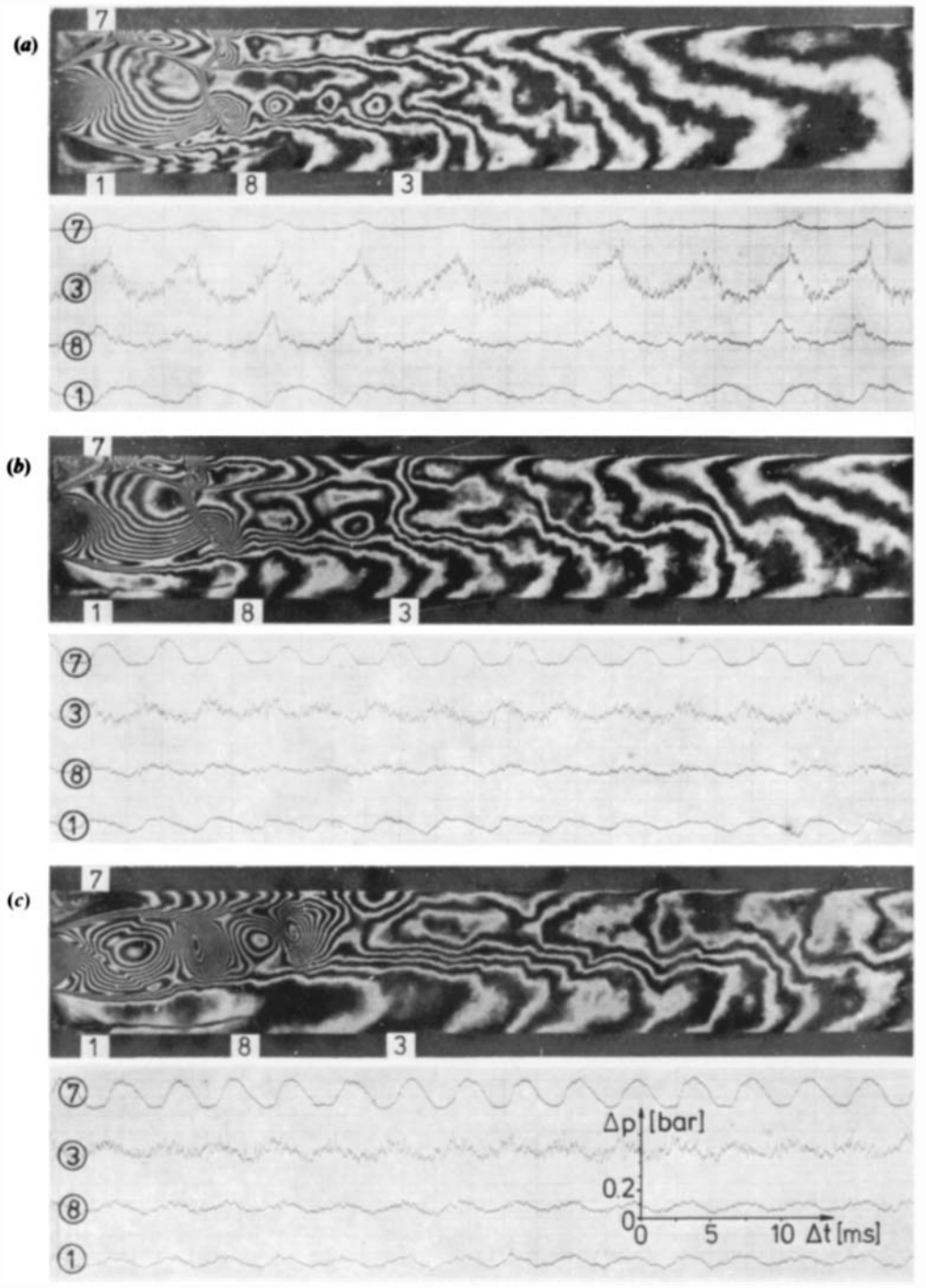

FIGURE 6. Interferograms of asymmetric flow patterns. $\phi = 0{\cdot}4$, $L = 240$ mm. (*a*) $p_e/p_a = 0{\cdot}42$, (*b*) $p_e/p_a = 0{\cdot}48$, (*c*) $p_e/p_a = 0{\cdot}488$.